SUPPORTING INFORMATION

EXPERIMENTAL METHODS:

Protein Purification: Full-length and fragments of HopPmaL from *Pseudomonas syringae* pv. maculicola str. ES4326 (gi|19071504|) and HopAB1 from *P. syringae* pv. phaseolicola str. 1448A ($HopAB1_{Pph1448a}$, gi |71725172|) were cloned into the expression plasmid p15TvLic, and the plasmid was transformed into *E. coli* BL21(DE3)-RIL or BL21(DE3)-RIPL (Stratagene). Following solubility assessment in test expression experiments, 1 L of *E. coli* cells containing the HopAB fragments were grown for x-ray crystallography or NMR; for X-ray crystallography, selenomethione-enriched protein was produced following growth at 18°C of cells in SeMet high-yield media (Shanghai Medicilon).

Briefly, for crystal structure determination, cells were grown at 37°C to an OD_{600} of 1.0 and induced overnight with IPTG at a temperature of 18°C. Cell pellets were then dissolved in 500 mM NaCl, 20 mM HEPES (pH 7.5), 0.5 mM TCEP and 5 mM imidazole and lysed by sonication and centrifuged to remove cell debris. Proteins were isolated from the lysates by batch nickel affinity chromatography (Qiagen), followed by washing the beads extensively (~50 column volumes) of this buffer plus 30 mM imidazole. Protein was eluted with 250 mM imidazole in this same buffer until no further protein could be eluted from the beads. However, the hexahistidine tag was not cleaved from the protein; instead the purified protein was dialyzed overnight with the lysis buffer

at 4°C, and the next day the dialyzed protein was concentrated to ~20-25 mg/ml and used for crystallization trials.

Samples for screening by NMR spectroscopy were purified from *E. coli* cells grown overnight at 37°C on auto-inducing minimal M9 media (*1*) containing $^{15}NH_4Cl$ as the nitrogen source and 5 g/L glucose and 2 g/L lactose as the carbon source, supplemented with $ZnSO_4$, thiamine, and biotin. Frozen cell pellets were thawed in 500 mM NaCl, 20 mM Tris, 5 mM imidazole (pH 8.0) and lysed by sonication. The proteins were extracted from the lysates by batch nickel affinity chromatography (Qiagen), followed by washing the beads three times with five column volumes of 500 mM NaCl, 20 mM Tris (pH 8.0), 30 mM imidazole. Protein was eluted with five column volumes of 500 mM imidazole in this same buffer. Aliquots of the purified proteins were dialysed against different NMR screening buffers and ^{15}N-^{1}HSQC spectra were acquired for each condition. For the 2D ^{15}N-^{1}H HSQC spectra shown, proteins were dialysed into a buffer containing 450 mM NaCl, 10 uM $ZnSO_4$, 10 mM DTT, 0.01 % NaN_3, 1 mM benzamidine and 95% H_2O/5% D_2O; samples of HopPmaL[1-138], HopPmaL[281-385] and HopPmaL[232-385] also contained 10 mM sodium acetate, pH 5.0, the sample of $HopAB1_{Pph1448A}$[1-90] also contained 10 mM MOPS, pH 6.5, and the sample of HopPmaL[218-307] also contains 10 mM Bis-Tris pH 6.0.

For NMR structure determination of HopPmaL[281-385] and $HopAB1_{Pph1448}$[220-320], *E. coli* cells were grown in 0.5 L of 2X M9 minimal medium containing $^{15}NH_4Cl$ and ^{13}C-glucose as the sole nitrogen and carbon source, respectively and supplemented with $ZnSO_4$, thiamine, and biotin. Cells were grown at 37°C to an OD_{600} of 1.0, followed by adding 1 mM isopropyl β-D-thiogalactoside (IPTG). The

temperature was reduced to 15 °C, and cells grew overnight before harvesting. Protein purification of the doubly-labeled proteins is the same as described for NMR screening but the hexahistidine tag was cleaved with TEV protease and the mixture passed through a nickel affinity column. The purified protein was concentrated, and buffer was exchanged by ultrafiltration and dilution/reconcentration into the NMR buffer containing 10 mM Tris (pH 7.0), 300 mM NaCl, 10 mM DTT, 1 mM benzamidine, 0.01% NaN_3, 1 x inhibitor cocktail (Roche Applied Science), 95%H_2O/5% D_2O.

The cytoplasmic domain (residues 268-615) of the *Arabidopsis thaliana* protein BAK1 (gi 18418211) was cloned into the expression vector pET28GST-LIC, which contains sequences for Glutathione S-transferase (GST), a hexahistidine affinity tag and a thrombin cleavage site upstream of the cloned gene (see www.sgc.utoronto.ca/SGC-WebPages/Vector.../ pET28GST-LIC.pdf). The plasmid was transformed into *E. coli* BL21(DE3)-RIL (Strategene). Following solubility tests, 1 L of *E. coli* cells containing this BAK1 plasmid were grown in l L LB and induced at an OD of 0.8 for 4.5 hours at 30°C. Cell pellets were then dissolved in 20 mM HEPES 7.5, 300 mM NaCl, 5% glycerol, 0.5 mM TCEP, a home-made protease inhibitor cocktail (containing 0.1 M Benzamidine and 0.05 M PMSF dissolved in absolute ethanol as a 500X stock), and 1 mM sodium pyrophosphate, and centrifuged to remove cell debris. Proteins were isolated from the lysates by batch affinity chromatography with glutathione Sepharose 4B (GE Healthcare), followed by washing the beads extensively with this buffer to remove unbound cell extract. Protein was eluted with 9 column volumes of 50 mM Tris 8.0, 0.2 M NaCl and 10 mM reduced glutathione. Protein then was exchanged into the lysis

buffer and concentrated to 25 mg/ml and stored by flash freezing small aliquots in liquid N_2.

Protein Crystallization: Crystallization trials were performed at room temperature using hanging-drop vapor diffusion with an optimized sparse matrix crystallization screen (*2*). HopPmaL fragments spanning from residue 54 to 232 (HopPmaL[54-232]) and from 135 to 273 (HopPmaL[135-273]) were crystallized only after use of the partial proteolysis technique (*3*). HopPmaL[54-232] was concentrated to 25 mg/ml, and the HopPmaL[54-232] crystal used for data collection was grown in a crystallization liquor containing 100 mM HEPES pH 7.5, 100 mM sodium chloride, 1.6M ammonium sulphate and 0.02 mg/ml thermolysin. HopPmaL[135-273] was concentrated to 22 mg/ml, and the crystal used for data collection was grown in a crystallization liquor containing 0.1M Bis-Tris pH6.5, 1.5M ammonium sulfate and 0.03 mg/ml chymotrypsin. Prior to data collection, crystals were cryoprotected using Paratone-N oil (Hampton Research) and flash-frozen in liquid nitrogen.

Data Collection, Structure Determination and Refinement : The HopPmaL[54-232] and HopPmaL[135-273] structures were solved using crystals derived from selenomethionine-enriched protein with SAD phasing using the anomalous signal collected from APS beamline 19-ID using a peak wavelength of λ=0.97942 Å. Diffraction data were integrated and scaled using HKL-2000 (*4*). Positions of heavy atoms were found using SHELXD (*5*), followed by solvent flattening using SHELXE (*6*), which was in turn used to automatically build an initial model using ArpWARP (*7*),

which was all used within the CCP4 program suite (*8*). The model was then improved by alternate cycles of manual building and water-picking using COOT (*9*) and restrained refinement against a maximum-likelihood target with 5% of the reflections randomly excluded as an R_{free} test set. These refinement steps were performed using REFMAC (*10*) in the CCP4 program suite, however additional refinements using TLS parameterization (*11, 12*) within CCP4, and Phenix.refine from the PHENIX crystallography suite (*13*) were also performed. The final model for each contains a single molecule of the HopPmaL Pto kinase-binding domain, representing residues 139-217 for HopPmaL[54-232] plus thermolysin, and residues 140-217 for HopPmaL[135-273] plus chymotrypsin; the final models were refined to an R_{work} and R_{free} of 18.6% and 21.8% for the thermolysin structure and 19.0% and 21.6% for the chymotrypsin structure, respectively**.** Data collection, phasing and structure refinement statistics for the HopPmaL crystal structures are summarized in Table S1. The Ramachandran plot generated by PROCHECK (*14*) showed very good stereochemistry overall with all residues in the most favored and additional allowed regions. HopPmaL[54-232] and HopPmaL [135-273] are target APC40104.6 and APC40132.2 of the Midwest Center for Structural Genomics, respectively.

NMR Spectroscopy: The NMR experiments were carried out at 25°C on either a Bruker Avance 600 or 800 MHz NMR Spectrometer equipped with cryogenic probes. ^{15}N T_1 and T_2 relaxation data were acquired using pseudo-2D ^{15}N-edited relaxation experiments on a Bruker Avance 600 MHz NMR Spectrometer at 25° (*15*). All 3D spectra employed non-uniformly sampling scheme in the indirect dimensions and were reconstructed by multi-dimensional decomposition software MDDNMR (*16*) (*17*),

interfaced with NMRPipe (*18*). The automated program FAWN (*19*) was used for the backbone assignments from HNCO, CBCA(CO)NH, HBHA(CO)NH, HNCA, and ^{15}N-edited NOESY-HSQC spectra. Aliphatic side chain assignments relied on (H)CCH-TOCSY and H(C)CH-TOCOSY spectra (*20, 21*). Aromatic ring resonances were assigned using 3D ^{13}C-edited NOESY spectra. Stereospecific valine and leucine methyl assignments were obtained as described (*22*) on the basis of the ^{13}C-^{13}C one-bond couplings in a high resolution 2D ^{1}H-^{13}C HSQC spectrum of 7%- ^{13}C, 100%- ^{15}N HopPmaL[281-385] and HopAB1$_{Pph1448a}$[220-320]. Nearly complete resonance assignments for HopPmaL[281-385] (98.5% backbone, 97.5% side-chain) were obtained. For HopAB1$_{Pph1448a}$[220-320], a total of 81 of the 94 expected backbone peaks were observed in the ^{15}N-^{1}H HSQC recorded at 25° and pH 7.0. The thirteen missing amide resonances are Gly221, Leu222, His235, Asn236, His237, Ser238, Ile267, Met 268, Ser269, Leu270, Leu273, Val301 and Thr319. Ninety-one percent of the C and H resonances for all side chains have been assigned.

NMR Structure Calculation: Distance restraints for structure calculations were derived from cross-peaks in ^{15}N-edited NOESY-HSQC (τ_m = 100 ms), ^{13}C-edited aliphatic and aromatic NOESY-HSQC in H_2O (τ_m = 100 ms) respectively. NOE peaks were picked with intensities using the program SPARKY (Goddard and Kneller 2003, http://cgl.ucsf.edu/home/sparky). Initial structure calculations were performed using the program CYANA 3.0 integrated with the noeassign module for automated NOE assignments (*23*). A total of 144 phi and psi torsion angle restraints for HopPmaL[281-385] and 136 phi and psi torsion angle restraints for HopAB1$_{Pph1448a}$[220-320] were

derived from the program TALOS+ (*24*). Hydrogen bond restraints were applied only for the helical regions as judged by NOE patterns and chemical shifts and supported by TALOS+. A total of 94.0% and 95.8% of NOESY peaks were assigned for HopPmaL[281-385] and HopAB1$_{Pph1448a}$ [220-320], respectively, in cycle 7. The quality of noeassign/CYANA calculation was assessed by NMR structure quality assessment scores (NMR PRF scores) (*25*). Recall, Precision, F-measure and DP scores were 0.926, 0.950, 0.938, 0.779, respectively, for HopPmaL[281-385], and 0.942, 0.919, 0.930 and 0.738, respectively, for HopAB1$_{Pph1448a}$ [220-320]. The best 20 of 100 CYANA structures from the final cycle were subjected to restrained molecular dynamics simulation in explicit water by the program CNS (*26, 27*). The final structures were inspected by PROCHECK (*28*) and MolProbity (*29*) using the NESG validation software package PSVS (*30*). The validation reports are accessible at www.nesg.org. HopPmaL[281-385] and HopAB1$_{Pph1448a}$ [220-320] are target PsT2A and PsT3A of the Northeast Structural Genomics Consortium, and target APC40104.5 and APC40132.4 of the Midwest Center for Structural Genomics, respectively. Structures were visualized using the program MOLMOL (*31*) and Pymol (http://pymol.sourceforge.net, Delano Scientific).

REFERENCES

1. Studier, F. W. (2005) *Protein Expr Purif 41*, 207-34.
2. Kimber, M. S., Vallee, F., Houston, S., Necakov, A., Skarina, T., Evdokimova, E., Beasley, S., Christendat, D., Savchenko, A., Arrowsmith, C. H., Vedadi, M., Gerstein, M., and Edwards, A. M. (2003) *Proteins 51*, 562-8.
3. Dong, A., Xu, X., Edwards, A. M., Chang, C., Chruszcz, M., Cuff, M., Cymborowski, M., Di Leo, R., Egorova, O., Evdokimova, E., Filippova, E., Gu, J., Guthrie, J., Ignatchenko, A., Joachimiak, A., Klostermann, N., Kim, Y., Korniyenko, Y., Minor, W., Que, Q., Savchenko, A., Skarina, T., Tan, K.,

Yakunin, A., Yee, A., Yim, V., Zhang, R., Zheng, H., Akutsu, M., Arrowsmith, C., Avvakumov, G. V., Bochkarev, A., Dahlgren, L. G., Dhe-Paganon, S., Dimov, S., Dombrovski, L., Finerty, P., Jr., Flodin, S., Flores, A., Graslund, S., Hammerstrom, M., Herman, M. D., Hong, B. S., Hui, R., Johansson, I., Liu, Y., Nilsson, M., Nedyalkova, L., Nordlund, P., Nyman, T., Min, J., Ouyang, H., Park, H. W., Qi, C., Rabeh, W., Shen, L., Shen, Y., Sukumard, D., Tempel, W., Tong, Y., Tresagues, L., Vedadi, M., Walker, J. R., Weigelt, J., Welin, M., Wu, H., Xiao, T., Zeng, H., and Zhu, H. (2007) *Nat Methods 4*, 1019-21.

4. Otwinowski, Z., and Minor, W. (1997) in *Methods in Enzymology* pp 307-326.
5. Schneider, T. R., and Sheldrick, G. M. (2002) *Acta Crystallogr D Biol Crystallogr 58*, 1772-9.
6. Sheldrick, G. M. (2008) *Acta Crystallogr A 64*, 112-22.
7. Perrakis, A., Morris, R., and Lamzin, V. S. (1999) *Nat Struct Biol 6*, 458-63.
8. (1994) *Acta Crystallogr D Biol Crystallogr 50*, 760-3.
9. Emsley, P., and Cowtan, K. (2004) *Acta Crystallogr D Biol Crystallogr 60*, 2126-32.
10. Murshudov, G. N., Vagin, A. A., and Dodson, E. J. (1997) *Acta Crystallogr D Biol Crystallogr 53*, 240-55.
11. Winn, M. D., Murshudov, G.N. & Papiz, M.Z. (2003) in *Methods Enzymol.* pp 300-321
12. Winn, M. D., Isupov, M. N., and Murshudov, G. N. (2001) *Acta Crystallogr D Biol Crystallogr 57*, 122-33.
13. Afonine P.V., Grosse-Kunstleve R.W, and P.D, A. (2005) *CCP4 NEWSLETTER ON PROTEIN CRYSTALLOGRAPHY 42*.
14. Laskowski R A, M. M. W., Moss D S & Thornton J M (1993) *J. Appl. Cryst. 26*, 283-291.
15. Farrow, N. A., Muhandiram, R., Singer, A. U., Pascal, S. M., Kay, C. M., Gish, G., Shoelson, S. E., Pawson, T., Forman-Kay, J. D., and Kay, L. E. (1994) *Biochemistry 33*, 5984-6003.
16. Gutmanas, A., Jarvoll, P., Orekhov, V. Y., and Billeter, M. (2002) *J Biomol NMR 24*, 191-201.
17. Orekhov, V. Y., Ibraghimov, I., and Billeter, M. (2003) *J Biomol NMR 27*, 165-73.
18. Delaglio, F., Grzesiek, S., Vuister, G. W., Zhu, G., Pfeifer, J., and Bax, A. (1995) *J Biomol NMR 6*, 277-93.
19. Lemak, A., Gutmanas, A., Chitayat, S., Karra, M., Fares, C., Sunnerhagen, M., and Arrowsmith, C. H. *J Biomol NMR 49*, 27-38.
20. Bax, A., Vuister, G. W., Grzesiek, S., Delaglio, F., Wang, A. C., Tschudin, R., and Zhu, G. (1994) *Methods Enzymol 239*, 79-105.
21. Kay, L. E. (1997) *Biochem Cell Biol 75*, 1-15.
22. Neri, D., Szyperski, T., Otting, G., Senn, H., and Wuthrich, K. (1989) *Biochemistry 28*, 7510-6.
23. Guntert, P. (2004) *Methods Mol Biol 278*, 353-78.
24. Shen, Y., Delaglio, F., Cornilescu, G., and Bax, A. (2009) *J Biomol NMR 44*, 213-23.

25. Huang, Y. J., Powers, R., and Montelione, G. T. (2005) *J Am Chem Soc 127*, 1665-74.
26. Brunger, A. T., Adams, P. D., Clore, G. M., DeLano, W. L., Gros, P., Grosse-Kunstleve, R. W., Jiang, J. S., Kuszewski, J., Nilges, M., Pannu, N. S., Read, R. J., Rice, L. M., Simonson, T., and Warren, G. L. (1998) *Acta Crystallogr D Biol Crystallogr 54*, 905-21.
27. Linge, J. P., Williams, M. A., Spronk, C. A., Bonvin, A. M., and Nilges, M. (2003) *Proteins 50*, 496-506.
28. Laskowski, R. A., Rullmannn, J. A., MacArthur, M. W., Kaptein, R., and Thornton, J. M. (1996) *J Biomol NMR 8*, 477-86.
29. Lovell, S. C., Davis, I. W., Arendall, W. B., 3rd, de Bakker, P. I., Word, J. M., Prisant, M. G., Richardson, J. S., and Richardson, D. C. (2003) *Proteins 50*, 437-50.
30. Bhattacharya, A., Tejero, R., and Montelione, G. T. (2007) *Proteins 66*, 778-95.
31. Koradi, R., Billeter, M., and Wuthrich, K. (1996) *J Mol Graph 14*, 51-5, 29-32.
32. Thompson, J. D., Gibson, T. J., and Higgins, D. G. (2002) *Curr Protoc Bioinformatics Chapter 2*, Unit 2 3.

Table S1: Data Collection and Refinement Statistics for the HopPmaL Pto-binding domain

	HopPmaL[54-232] (thermolysin)	**HopPmaL[135-273] (chymotrypsin)**
Data collection		
Space group	*P41212*	*P41212*
Cell dimensions		
a, *c* (Å)	57.3, 55.7	57.4, 54.8
Wavelength (Å)	0.97942	0.97942
Resolution (Å)	50-1.75 (1.78-1.75)	50-1.65(1.68-1.65)
R_{merge} (%)[a]	0.071(0.428)	0.080(0.501)
$I/\sigma I$	43.4(3.9)	42.1(3.6)
Completeness (%)	99.9(100.0)	99.9(100.0)
Redundancy	9.2(9.4)	9.3(9.5)
Refinement		
Resolution (Å)	25.6-1.80	25.7-1.70
No. reflections	9038(432)	10558(510)
R_{work} (%)[b]	18.6	19.0
R_{free} (%)[c]	21.8	21.6
No. atoms		
Protein	673	682
Water	71	82
Other	15	19
B-factors (Å^2)		
Overall	23.8	21.4
Protein	22.6	19.9
Water	30.8	29.1
Other	43.9	43.1
r.m.s. deviations		
Bond lengths (Å)	0.007	0.008
Bond angles (°)	1.0	1.1
Ramachandran Plot		
% in Most Favored Regions	96.5	96.5
% in Additionally Allowed Regions	3.5	3.5
% in Disallowed Regions	0.0	0.0

Notes:
Values in parentheses are for the highest-resolution shell.

[a] $R_{merge} = \sum_{hkl} \left| I - \langle I \rangle \right| / \sum_{hkl} I$

[b] $R_{work} = \sum \left| F_{obs} - F_{calc} \right| / \sum \left| F_{obs} \right|$, where F_{obs} and F_{calc} are the observed and the calculated structure factors, respectively.

[c] R_{free} calculated using 5% of total reflections randomly chosen and excluded from the refinement

Table S2. Structural statistics for the ensemble calculated for the HopPmaL[281-385] and HopAB1$_{Pph1448}$[220-320] solution structures

	HopPmaL[281-385]		**HopAB1$_{Pph1448}$[220-320]**	
Distance restraints[a]				
All	2705		2079	
Intra-residue (i = j)	415		351	
Sequential (|i-j| = 1)	694		468	
Medium range (2 ≤ |i-j| ≤ 4)	894		678	
Long range (|i-j| > 4)	702		582	
Hydrogen bonds	30x2		27x2	
Dihedral angle restraints[b]				
All, ϕ, φ	144, 72, 72		136, 68, 68	
r.m.s.d from experimental restraints				
Distance (Å)	0.0189 ± 0.0008		0.0150 ± 0.0009	
Dihedral angle (°)	0.1278 ± 0.0941		0.1700 ± 0.0796	
r.m.s.d from idealized covalent geometry				
bond (Å)	0.0146 ± 0.0002		0.0144 ± 0.0002	
bond angles (°)	0.9623 ± 0.0135		0.9292 ± 0.0186	
CNS energy (kcal/mol)				
Total	-2832 ± 106		-2775 ± 61	
Van der Waals	-643 ± 22		-633 ± 10	
Electrostatic	-3647 ± 91		-3466 ± 52	
r.m.s.d from mean structure[b]				
Backbone atoms	0.28 ± 0.05		0.39 ± 0.05	
All heavy atoms	0.58 ± 0.06		0.82 ± 0.04	
Ramachandran plot (%)[b]				
Residues in most favored regions	95.1		93.4	
Residues in additional allowed regions	4.9		6.6	
Global quality scores[c]	Raw	Z-score	Raw	Z-score
Verify3D	0.34	-1.93	0.35	-1.77
ProsaII	0.80	0.62	0.88	0.95
Procheck (phi-psi)[b]	0.08	0.63	0.16	0.94
Procheck (all)[b]	-0.25	-1.48	-0.09	-0.53
MolProbity clash	16.45	-1.30	14.33	-0.93

NMR structure consists of an ensemble of the 20 lowest energy structures out of 100 calculated.

[a]No distance restraint was violated by > 0.5 Å and no dihedral restraint was violated by > 5° in either ensemble of 20 lowest energy structures

[b]Rmsd values for residues 308-384 of HopPmaL[281-385] and residues 239-267, 271-315 of HopAB1$_{Pph1448}$[220-320].

[c]Calculated from NESG PSVS program (Bhattacharry et al. 2007)

Figure S1. (A) Superimposition of AvrPtoB[120-205] residues 124-200 (from PDB 3HGK)(green cartoon) with HopPmaL residues 139-217 (cyan cartoon, left panel). As with Figure 2, N and C represents the N- and C-terminus of AvrPto[120-205], while N' and C' represents the N- and C-terminus of the HopPmaL fragment. (B) Close-up of the putative Pto-binding region of HopPmaL[139-217] with residues expected to bind Pto based on the AvrPtoB[120-205] structure shown in a stick representation and labeled.

Figure S2. (A) Superimposition of the 20 lowest energy structures of HopPmaL[281-385] and HopAB1$_{Pph1448a}$[220-320]. Regions of secondary structure are labeled. (B) Superimposition of residues 305-385 and 237-320 from the NMR structures of HopPmaL [281-385] and HopAB1$_{Pph1448a}$[220-320], respectively. N- and C-termini are labeled as are the secondary structure elements. Residues potentially involved in binding a target kinase are shown in a stick representation and labeled; these residues are similar to those shown in Figure 2, and lie within helix C, D and the loop between these two helices. Colouring of the different molecules is similar to that used in Figure 1 and 2.

Figure S3. Sequence alignment of of HopPmaL[308-385] (HopPmaL_cterm) and HopAB1$_{Pph1448a}$[239-316](HopAB1_1448a) with the middle domains of other HopAB alleles and the N-terminal Pto-binding domains of AvrPtoB (AvrPtoB_3HGL) and HopPmaL (HopPmaL_nterm), generated using ClustalX (*32*). The positions of helices (red ovals) and loop regions (black lines) in the HopPmaL C-terminal and N-terminal domain are shown above and below the sequence alignment, respectively. Helices are labeled using the nomenclature described earlier, where nt and ct refer to the N-terminal

and C-terminal domains of HopPmaL, respectively. Brown boxes above the sequence of the HopPmaL C-terminal domain indicate residues in HopPmaL[281-385] which were buried in the hydrophobic core, showing limited conservation with the N-terminal Pto-binding domain. Green boxes below the sequence of the HopPmaL N-terminal domain represent residues of the AvrPtoB N-terminal domain whose side chains interact with the Pto kinase. Other sequences are derived from HopAB alleles from *Pseudomonas savastanoi* str. ITM317 (virPphAPsv, g.i.|75401898|), *P. syringae* pv. glycinea str. 49a/90 (virPphAPgy, g.i. |75401901|), *P. syringae* pv. syringae str. B728a (HopAB1_B728a, g.i. |66047883|), *Pseudomonas avellanae* (HopAB_avellanae, g.i. 146327848), *P. syringae* pv. tomato str. JL1065 (HopAB3_Psesm, g.i. |94717621|), *P. syringae* pv. tomato str. T1 (HopAB3_T1, g.i. |213970380|) and *P. syringae* p.v. theae (HopAB3_theae, gi. | 146327850|).

Figure S4. Titration of GST-BAK1[268-615] into a sample of 0.2 mM ^{15}N-labeled HopPmaL[281-385]. Three ^{15}N-^{1}H HSQC spectra are shown at HopPmaL/BAK1 ratios of (A) 1:0.28, (B) 1:0.56 and (C) 1:1.4. Prior to titration, both proteins were dialysed into a buffer containing 10 mM Tris 7.0 and 300 mM NaCl.

Figure S5. (A) Representative ^{15}N-^{1}H HSQC spectrum for HopPmaL[1-138] (B) Representative ^{15}N-^{1}H HSQC spectrum for HopAB1$_{Pph1448a}$[1-90]. (C) Representative ^{15}N-^{1}H HSQC spectrum for HopPmaL[218-307].

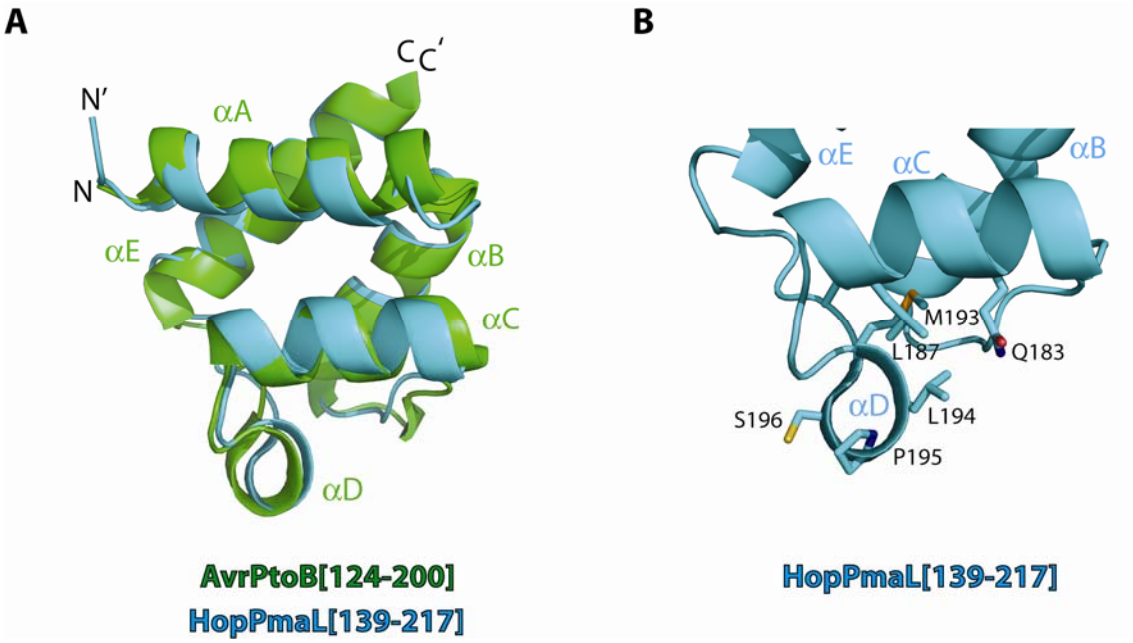
A
C
C′
N′
N
αA
αE
αB
αC
αD
AvrPtoB[124-200]
HopPmaL[139-217]
B
αE
αC
αB
M193
L187
Q183
αD
S196
L194
P195
HopPmaL[139-217]

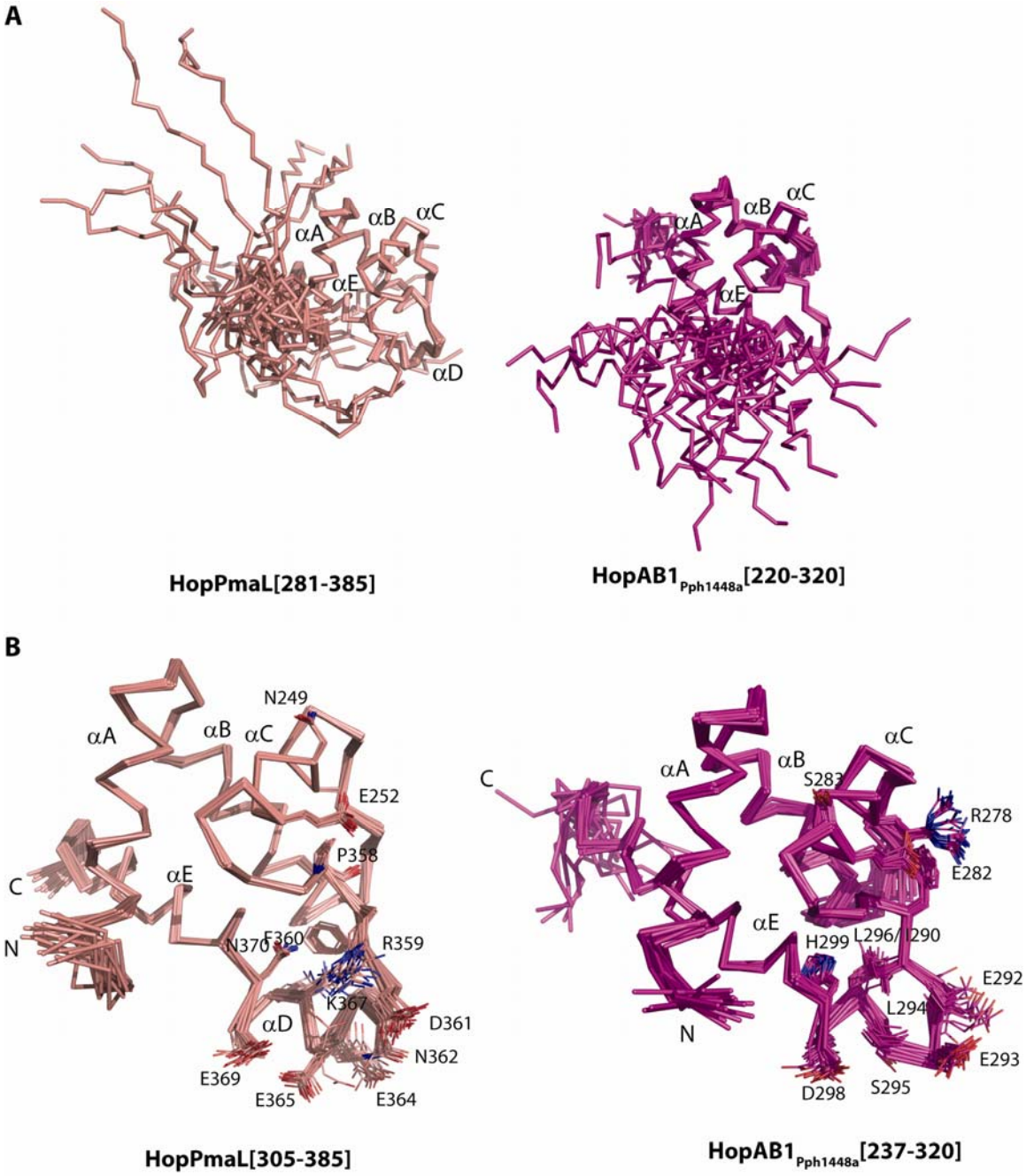
A
αA
αB
αC
αE
αD
HopPmaL[281-385]
αA
αB
αC
αE
HopAB1Pph1448a[220-320]
B
N249
αA
αB
αC
E252
P358
C
αE
N
N370
E360
R359
K367
αD
D361
N362
E369
E365
E364
HopPmaL[305-385]
C
αA
αB
αC
S283
R278
E282
αE
H299
L296/L290
E292
L294
N
E293
D298
S295
HopAB1Pph1448a[237-320]

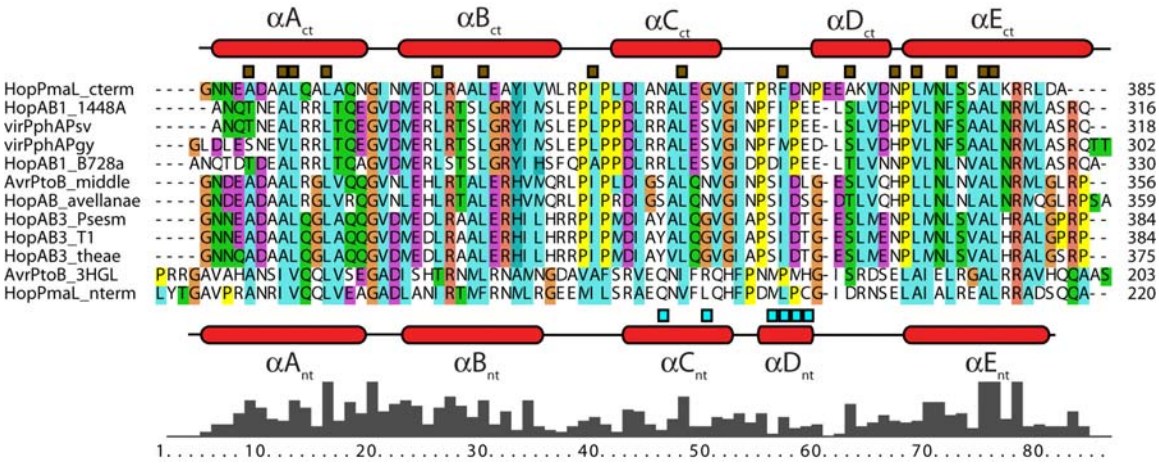
αA_ct
αB_ct
αC_ct
αD_ct
αE_ct
HopPmaL_cterm
HopAB1_1448A
virPphAPsv
virPphAPgy
HopAB1_B728a
AvrPtoB_middle
HopAB_avellanae
HopAB3_Psesm
HopAB3_T1
HopAB3_theae
AvrPtoB_3HGL
HopPmaL_nterm
385
316
318
302
330
356
359
384
384
375
203
220
αA_nt
αB_nt
αC_nt
αD_nt
αE_nt
1. . . . . 10. . . . . 20. . . . . 30. . . . . 40. . . . . 50. . . . . 60. . . . . 70. . . . . 80. . . . .

A.

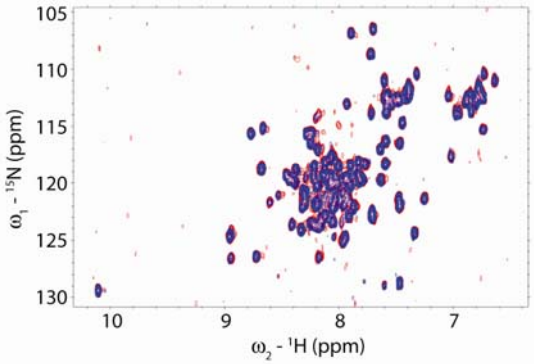
105
110
115
120
125
130
10
9
8
7
ω1 - 15N (ppm)
ω2 - 1H (ppm)

B.

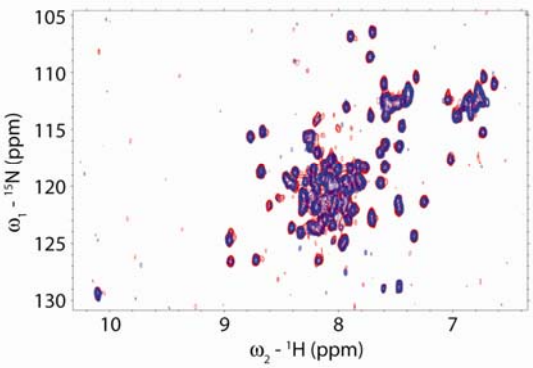
105
110
115
120
125
130
10
9
8
7
ω1 - 15N (ppm)
ω2 - 1H (ppm)

C.

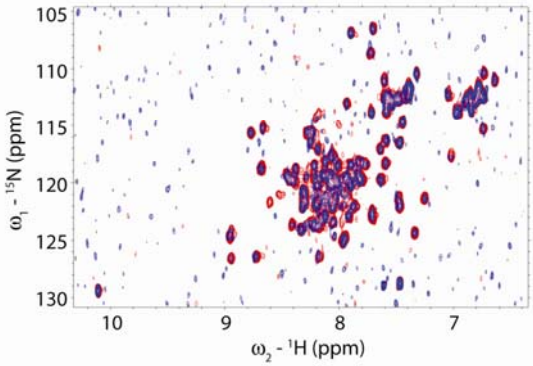
105
110
115
120
125
130
10
9
8
7
ω1 - 15N (ppm)
ω2 - 1H (ppm)

A. HopPmaL[1-138]

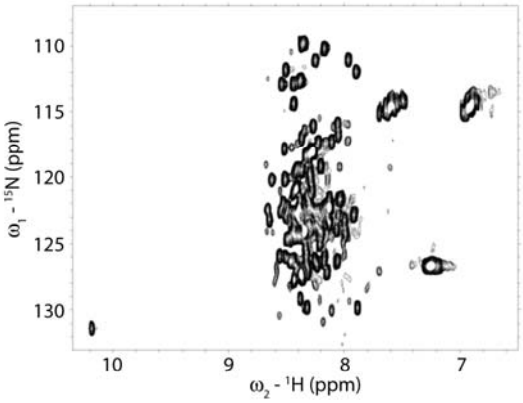

B. HopAB1$_{Pph1448a}$[1-90]

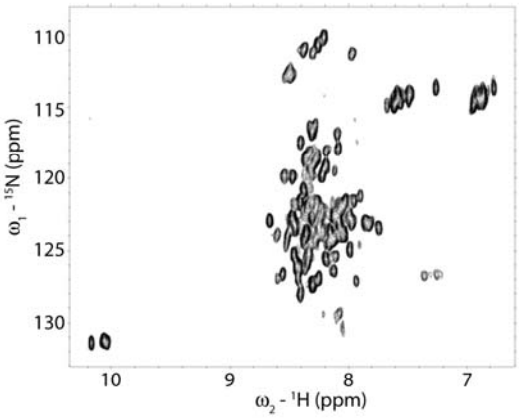

C. HopPmaL[218-307]